Peak Width and Reagent Dispersion in Flow Injection Analysis

PEAK WIDTH AND REAGENT DISPERSION IN FLOW INJECTION ANALYSIS

JULIAN F. TYSON

Department of Chemistry, University of Technology, Loughborough, Leicestershire, LE11 3TU (Great Britain)

(Received 6th September 1985)

SUMMARY

Accurate equations are derived for relating peak width to injected concentration for single-line and merging-stream manifolds in which a well stirred mixing chamber is used to generate concentration gradients. The consequences of making an approximation to produce a linear relationship between peak width and the natural logarithm of the injected concentration are evaluated and shown to have little practical effect. The concept of reagent dispersion coefficient, D^R, is used in certain derivations and a relationship between this and the conventional dispersion coefficient is derived and investigated experimentally. The use of D^R to evaluate the likely performance of other flow-injection modes is illustrated for the calculation of reagent-to-sample concentration ratios and the case of reversed f.i.a. (reagent injected into sample carrier stream). An extension of the usual peak-width method is in f.i.a. described; a low-dispersion coefficient manifold is used and the product concentration profile is monitored. The analytical information in the double peaks obtained is discussed and illustrated for the peak-width mode by the injection of copper(II) ions (1.6×10^{-6}—0.16 M) into a carrier stream of 10^{-4} M EDTA. The single well stirred mixing chamber model is used as a basis for the evaluation of the results and is applied to discussion of other manifolds not containing a real mixing chamber, in particular for the calculation of peak base-widths.

Although the most commonly used quantitative parameter in flow injection analysis (f.i.a.) is the peak maximum, the originators of the technique, Růžička and Hansen have shown that analytical information is available from other properties of the response curve (see, e.g. [1]). The peak maximum has the advantage of being very easily located on the recording of detector response vs. time and its use is thus more in keeping with the general philosophy of f.i.a. than, for example, peak area or a point on the peak tail which require additional signal-processing devices. However, the use of peak height suffers from the same limitations as for conventional steady-state analyses, namely that an upper limit to the working range is set. This may be due to the response being "off-scale" or into a very non-linear part of the calibration function or because there is insufficient reagent to produce the appropriate amount of product.

These disadvantages may be overcome if the width of the peak is measured. Under appropriate circumstances, the points between which the peak

width is to be measured may be identified accurately using only a chart recorder. Previously, such methods have been referred to as "titrations" [2], "pseudotitrations" [3], "variable-time kinetic" methods [4] and "scale expansion" methods [5]. Some of these terms are misleading and all obscure the basis of the quantification, namely measurement of peak width, which must be confusing to newcomers to the technique. It is proposed here that all methods encompassed by the terminology above be known as "peak-width" methods and that these form a subset of all "time-based" methods in f.i.a. This latter set would also include methods based on "electronic dilution" [6], "gradient calibration" (both decreasing [6] and increasing [7]), "stopped flow" [8], "gradient scanning" [9] and "zone sampling" [10] amongst others.

In order to obtain a relationship between peak width and the concentration of the material injected, the concentration/time (C, t) equations for the rise and fall curves must be known. If the C, t equations are exponentials, as produced by a well-stirred mixing chamber, then the peak width is related to the logarithm of the concentration. Two groups of workers have previously derived peak-width equations, several of which are inaccurate. Růžička and co-workers [2, 6] assumed that the injected sample volume was instantly dispersed throughout the mixing chamber and then washed out. This is the tanks-in-series model for dispersion behaviour [11] with the number of tanks reduced to one and does not correspond to the situation, often adopted in practice, in which a real mixing chamber is introduced into the manifold and the sample slug flows into the tank. It is also possible in practice for the injected volume to be larger than the tank volume, a situation not covered by this version of the tanks-in-series model. Olsen et al. [6] considered that, for a system without a real mixing chamber, the dispersion produced was equivalent to wash out from a tank comprising the reactor volume plus half the injected volume. This situation is possibly covered better by the "one-tank" model but examination of their experimental results shows the rise time to occupy a significant proportion of the total peak time, at variance with the prediction of an infinitely fast rise time. This paper [6] also corrects an error in the equivalence condition made in the earlier paper [2], but perpetuates the hidden approximation in deriving the equation for the single-line manifold.

Pardue and Fields [4] adopted a model based on slug flow up to a well stirred tank, but make unnecessary approximations in deriving their final peak-width equation and also perpetuate the error in the equivalence condition.

Here, exact equations are derived for the passage of an injected slug through a well stirred mixing chamber for a single-line manifold for the conditions (a) no reagent in the carrier stream and (b) reagent in the carrier stream. The equations are also applied to a merging stream manifold in which the dispersed sample zone is merged with a stream of reagent. The potential of the peak-width method for extending the working range of a technique,

particularly when a manifold with a low dispersion coefficient is used and the product of the reaction is followed, is demonstrated. The derivation of the equations makes use of the concept of reagent dispersion coefficient and the usefulness of this concept in other f.i.a. situations is discussed.

DERIVATION OF PEAK-WIDTH EQUATIONS

Physical dispersion in a well stirred mixing chamber

The manifold and underlying assumptions are shown in Fig. 1A. An abbreviated version of this derivation has been given [12]. A fuller version is given in Appendix 1 together with some other useful equations relating to this model [13]. The resulting equation (all symbols are explained in Table 1) is

$$\Delta t = (V/u^s) \ln [(C^s_m/C') - 1] - (V/u^s) \ln (D - 1) \quad (1)$$

Thus the width of the peak is not directly proportional to the logarithm of the injected concentration but to the function $\ln [(C^s_m/C') - 1]$. The former relationship is only obtained if the approximation $C^s_m/C' \gg 1$ is valid and hence $(C^s_m/C') - 1 \approx C^s_m/C'$. The extent to which this approximation is valid will be discussed later.

Physical dispersion of sample and reagent

Just as the dispersion coefficient based on the injected sample material is given by

$$D = C^s_m/C^s_p \quad (2)$$

it is proposed that the reagent dispersion coefficient be defined by

$$D^R = C^R_m/C^R_p \quad (3)$$

These definitions are valid for any single-line manifold, of course, and can be extended to any point on the reagent or sample profile:

$$D_g = C^s_m/C^s_g \quad (4)$$

$$D^R_g = C^R_m/C^R_g \quad (5)$$

The concentrations involved are indicated in Fig. 2A.

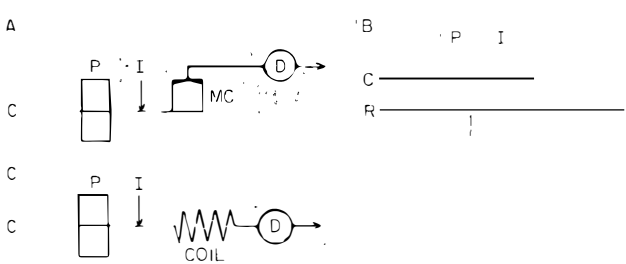

Fig. 1. Manifolds for peak-width methods: C, water carrier stream; D, detector; I, injector; MC, mixing chamber; P, pump; R, reagent stream. Manifolds A and B are hypothetical. It is assumed that the injected sample plug is not dispersed between I and MC nor is there any dispersion between MC and D, nor in D itself.

TABLE 1

List of symbols

Symbol	Definition
C	Concentration
C'	Concentration at which peak width is measured
C_{bl}	Concentration indistinguishable from baseline
C_{eq}	Concentration at equivalence point (before reaction)
C_g	Concentration at any point on dispersed profile
C_m	Steady-state concentration
C_p	Peak concentration
C^R	Reagent concentration
C^s	Sample concentration
D	Dispersion coefficient for injected material ($D = C^s_m/C^s_p$)
D^R	Dispersion coefficient for carrier stream material ($D^R = C^R_m/C^R_p$)
D_g	Dispersion coefficient for injected material at any point on peak profile
D^R_g	Dispersion coefficient for carrier stream material at any point on inverse peak profile
f^R	Fraction of total flow rate caused by merged reagent stream [$f^R = u^R/(u^R + u^s)$]
f^s	Fraction of total flow rate caused by merged sample stream [$f^s = u^s/(u^R + u^s)$]
R	Reagent (carrier stream material)
$R^{R/s}$	Ratio of reagent to sample concentrations (subscripts m and p also apply)
S	Sample (injected material)
t	Time
t_1, t_2	Time taken to reach C' on rising profile and falling profile, respectively
t_p	Time to reach peak maximum ($t_p = V_i/u$)
Δt	Peak-width ($\Delta t = t_2 - t_1$)
Δt_{eq}	Peak-width when $C' = C_{eq}$
Δt_b	Peak base width
u	Volumetric flow rate
u^R	Volumetric flow rate of reagent stream
u^s	Volumetric flow rate of injected sample carrier stream
V	Volume of mixing chamber
V_i	Volume injected
∂V	Hypothetical detector volume
∂V_r	Hypothetical volume of sample removed from ∂V and hypothetical volume of reagent replaced to account for sample and reagent dilution at point of measurement

In order to derive the relationship between D and D^R, it is first assumed that the concentration is monitored in a finite volume ∂V. This avoids the difficulties associated with considering concentrations at a point or in an infinitely thin slice across the tube. Secondly, it is assumed that a diluted sample concentration has been obtained in ∂V by replacement of a volume ∂V_r by an equal volume of reagent solution. The resulting concentrations of the sample and reagent are given by $C^s_g = C^s_m\,(\partial V - \partial V_r)/\partial V$ and $C^R_g = C^R_m\,\partial V_r/\partial V$, respectively. For the sample, substitution from Eqn. 4 gives $1/D_g = 1 - (\partial V_r/\partial V)$. For the reagent, substitution from Eqn. 5 gives $1/D^R_g = \partial V/\partial V_r$.

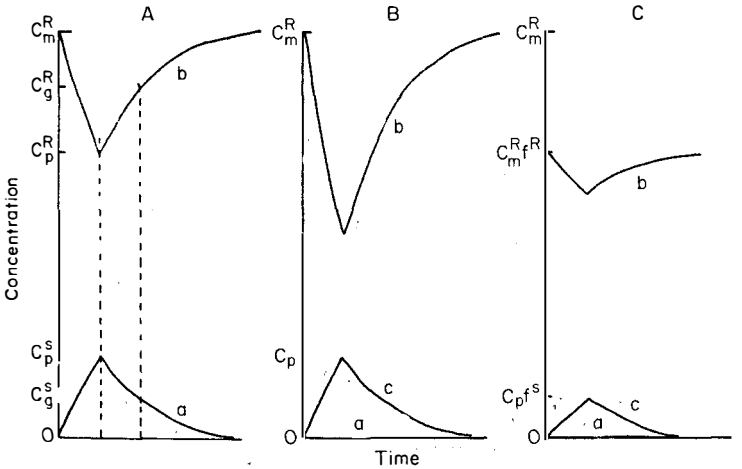

Fig. 2. Concentration profiles of dispersed sample and reagent without and with chemical reaction for C^R always greater than C^s. A, the sample (a) and reagent (b) profiles for manifold 1A with no chemical reaction; B, the sample (a), reagent (b) and product (c) profiles when chemical reaction occurs; C, the same profiles for manifold 1B in which C is a water carrier stream and R is the reagent carrier stream.

Reorganization of these last two equations gives $1/D_g = 1 - 1/D_g^R$ and $1/D_g^R = 1 - 1/D_g$. Thus

$$D_g = D_g^R/(D_g^R - 1) \tag{6a}$$

$$D_g^R = D_g/(D_g - 1) \tag{6b}$$

The corresponding equations for the dispersion coefficients at the peak maxima are obtained by dropping the subscript g. An experimental verification of Eqns. 6(a) and 6(b) will be described later, as will some other applications of the equations. The equations are in agreement with that derived previously for the well stirred mixing chamber model [13].

Chemical reaction between sample and reagent in a well stirred mixing chamber

If C^R is always greater than C^s across the profile (as shown in Fig. 2A), then the peak width of the product profile (Fig. 2B) will be as given in Eqn. 1 for the single-line manifold (Fig. 1A) and will be modified (Fig. 2C) by the inclusion of the flow rates of the sample carrier stream and merging reagent stream to account for the dilution at the confluence point, for the manifold shown in Fig. 1B:

$$\Delta t = (V/u^s) \ln [(C_m^s/C') - 1/f^s] - (V/u^s) \ln (D - 1/f^s) \tag{7}$$

The equation is derived in full in Appendix 2.

Taking the single-line manifold case first, if the dispersion produced is

such that $C^s > C^R$ in the profile centre (the reagent is in deficit, as shown in Fig. 3A), then there are points on the rising and falling profiles at which the concentrations are in the stoichiometric ratio for the reaction between R and S. Here it is assumed that this ratio is 1:1 (the full equations for a ratio $m:n$ are given in Appendix 4). These profiles represent the situation properly described as a "titration", as there are equivalence points on the rise and fall curves.

The concentration of reagent and sample at these points if reaction occurs, C_{eq}, may be found from either version of Eqn. 6. For example, from Eqn. 6(b), at an equivalence point $C^R_{eq} = C^s_{eq}$ for a 1:1 reaction

$$C^R_m/C^s_{eq} = (C^s_m/C^s_{eq})/[(C^s_m/C^s_{eq}) - 1]$$

thus $C^s_m/C^R_m = (C^s_m/C^s_{eq}) - 1$, and $C^s_m/C^s_{eq} = (C^s_m + C^R_m)/C^R_m$, so

$$C^s_{eq} = C^s_m C^R_m/(C^s_m + C^R_m) \tag{8}$$

As Eqn. (8) is derived from Eqn. 6, its validity is independent of the curve shape and shows that, provided all elements of the sample and reagent zones are subject to the same dispersion effects, the line joining the two equivalence points is parallel to the time axis. The peak width at the equivalence point, Δt_{eq}, is obtained by substituting C_{eq} for C' in Eqn. 1 and for C_{eq} from Eqn. 8. This gives

$$\Delta t_{eq} = (V/u^s) \ln (C^s_m/C^R_m) - (V/u^s) \ln (D - 1)$$
$$= (V/u^s) \ln C^s_m - (V/u^s) \ln C^R_m(D - 1) \tag{9}$$

Thus, without any approximation, Δt_{eq} is a linear function of $\ln C^s_m$. The corresponding equation for the manifold shown in Fig. 1B is derived in Appendix 3 and is

$$\Delta t_{eq} = (V/u^s) \ln [(C^s_m/C^R_m) - (u^R/u^s)] - (V/u^s) \ln [Df^R - (u^R/u^s)] \tag{10}$$

In the situation where the flow rates are equal ($u^R = u^s$), Eqn. 10 reduces to

$$\Delta t_{eq} = (V/u^s) \ln [(C^s_m/C^R_m) - 1] - (V/u^s) \ln [(D/2) - 1] \tag{11}$$

It should be noted that Δt_{eq} represents a real peak width only for the product profile (which has now become a double peak as shown in Fig. 3B) and represents a hypothetical width for the reagent and sample profiles (physical dispersion without chemical reaction). If the real reagent or sample profile is followed, as is often the case in reports of the application of this type of peak-width method in f.i.a., then there is a practical problem of locating the equivalence points. As they are at points in which the gradients of the profiles show the greatest change, this is often taken as the criterion for their location. It should also be noted that the equivalence concentration in the single-line manifold case is a function of the injected concentration and thus the corresponding concentration level of reagent or sample at the equivalence points varies with C^s_m. Thus selection of a single measurement level, as

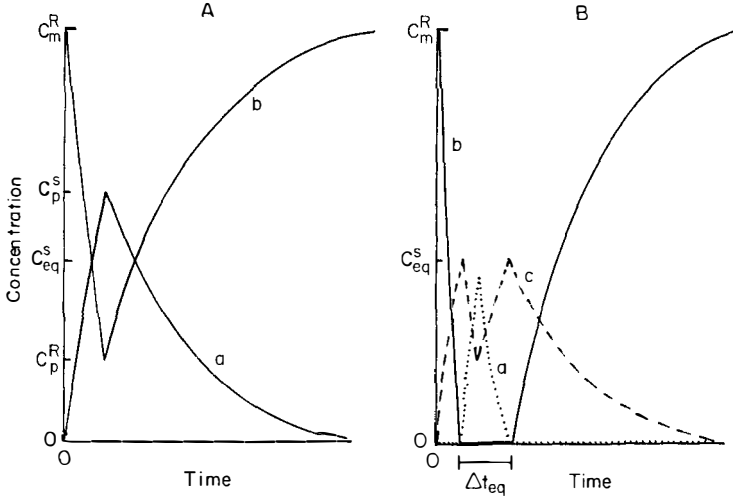

Fig. 3. Concentration profiles of dispersed sample and reagent without and with chemical reaction for C^S greater than C^R in the profile centre. A, The sample (a) and reagent (b) profiles for manifold 1A with no chemical reaction; B, the sample (a), reagent (b) and product (c) profiles when chemical reaction occurs.

is invariably done in practice, represents a further approximation in the method.

Equations 9—11 may also be used to calculate a limiting concentration for a given set of experimental conditions at which Δt_{eq} becomes zero and thus the "limit of detection" has been reached. However, the equations also clearly show that it is easy to arrange matters so that this limit is never reached. Putting $\Delta t_{eq} = 0$ for Eqn. 9, for example, shows that the limit is reached when $C_m^s/C_m^R = D - 1$. And thus, no matter how small the ratio C_m^s/C_m^R is, a peak width will be obtained provided that D is small enough. In practical terms, the easiest way to achieve this is to inject a sufficiently large volume. Such a volume is readily calculated from the equation $V_i = V \ln [D/(D - 1)]$ (Eqn. A1.7, Appendix 1) for any given volume of mixing chamber; substituting from the peak maximum version of Eqn. 6 gives

$$V_i = V \ln D^R \qquad (12)$$

This is a further example of the use of the reagent dispersion coefficient concept.

There is thus no reason to limit the concentration of the injected material to values greater than the concentration of the reagent in the carrier stream as seems to be common practice [14]. The larger the volume injected, the smaller the sampling frequency and so speed of analysis is a trade-off for decreasing the C_m^s/C_m^R ratio. This aspect will be discussed later.

It is suggested here that the full potential of the peak-width method is realised only with a single-line manifold of small dispersion coefficient in

which the concentration of the product is monitored. This produces doublet peaks as illustrated in Fig. 3B. There is then no difficulty in locating the equivalence points. The limit of detection is set by the ability of the detector to detect a product peak above the baseline noise. Furthermore, there is no need for the detector response to be linearly related to concentration and no need to maintain the same response parameters for each sample injected. An example in which the sample concentration was varied over five orders of magnitude is given later.

EXPERIMENTAL

Two types of experimental work are described. First, illustrative calculations based on some of the equations derived above are given, using, where appropriate, data based closely on results reported in the literature. Secondly, experiments illustrative of the validity and use of some of the above concepts are described.

Physical dispersion with no chemical reaction

Values of the appropriate parameters of V_i = 50 μl, V = 200 μl, u^s = 50 μl s^{-1} and C_m = 10 to 10 000 $\mu g\ l^{-1}$ were taken from Stewart and Rosenfeld [5] and used to calculate points for a plot of Δt vs. ln $[(C_m^s/C') - 1]$ and Δt vs. ln C_m^s. A linear regression analysis of the data was made. A value of C' was not given and was taken here to be 2 $\mu g\ l^{-1}$.

Reagent dispersion

The manifold shown in Fig. 1C was used in which P was a Gilson Minipuls-2 peristaltic pump, the injection valve was an Altex type 201-25 eight-port, double-loop (44 and 63 μl) valve, the coil was 100 cm of teflon tubing (0.71 mm i.d.) and the detector was a Pye-Unicam PU4020 u.v. detector for liquid chromatography incorporating an 8-μl flow cell. Peaks were recorded on a Pye-Unicam PM8251 chart recorder. The test solution was 10^{-4} M potassium nitrate, the wavelength was 200 nm and the flow rate was measured by collecting and weighing the detector effluent when distilled water was used as the carrier stream over intervals of ten minutes. The mean and 95% confidence interval were calculated with no correction for density.

With water as the carrier stream, 10^{-4} M potassium nitrate was injected from each loop and the resulting peaks were recorded at a chart speed of 300 mm min^{-1}. The carrier was changed to 10^{-4} M potassium nitrate, the chart recorder rewound and water injected from each loop at the same point on the chart as injections for the first experiment. Values of D_g and D_g^R were calculated from measurements taken directly from the chart recording (a linear absorbance/concentration relationship was assumed), the corresponding values of D_g^R and D_g were calculated from Eqns. 6(b) and 6(a), respectively, and linear regression was applied to the data. The 95% confidence intervals for the slope and intercept were also calculated.

A plot of D^R vs. D based on Eqn. 6 was constructed, as was a plot of C_m^R/C_m^s vs. D to illustrate the use of the reagent dispersion coefficient concept in calculating C_p^R/C_p^s ratios. The latter is necessary in conventional f.i.a. based on peak-height measurement to ensure an adequate excess of reagent over sample to drive the desired reaction to an appropriate extent.

To illustrate the use of some of the concepts described earlier to assess the features of reversed f.i.a. (reagent injected into sample carrier stream), calculations were done with values based on those of Johnson and Petty [15]: $V = 100\ \mu l$, $D = 5$ and $u = 33.3\ \mu l\ s^{-1}$.

Dispersion and chemical reaction

The manifold shown in Fig. 1C was used as described above except that one of the sample loops was replaced by a 500-μl loop. The carrier reagent stream was 10^{-4} M EDTA (disodium salt) and sample solutions covering the range 0.1—10 000 mg l^{-1} copper(II) (1.6×10^{-6}—0.16 M). The absorbance was monitored at appropriate wavelengths to obtain the double peaks of the type shown in Fig. 3B. This was necessary because reagent, sample and product all absorb to some extent over the usable wavelength range. The wavelengths used were 270 nm (0.1 mg l^{-1}), 340 nm (1, 10, 100 mg l^{-1}), 290 nm (1000 mg l^{-1}) and 320 nm (10 000 mg l^{-1}).

Values of the "mixing chamber volume" and dispersion coefficient for the experimental results obtained with the manifold (Fig. 1C) were estimated from the slope and intercept of the plot of Δt_{eq} against ln C_m^s. Some representative calculations of the sampling frequency for the low dispersion mode and the variation of C_{eq} with C_m^s for a given value of C_m^R of 10^{-4} M was calculated according to Eqn. 8.

RESULTS AND DISCUSSION

Physical dispersion with no chemical reaction

The results of the calculations based on Eqn. 1 are given in Table 2. The parameters of the linear regression for the plot of Δt vs. ln $[(C_m^s/C') - 1]$ were slope 3.999 s, intercept —5.036 s and correlation coefficient 0.999995; the values for the corresponding plot of Δt vs. ln C_m (the approximation commonly used) were slope, 4.081 s, intercept —8.414 s and correlation coefficient 0.999796. Values of Δt were calculated to 3 significant figures as were the values of the logarithmic functions. These results show that the approximation of neglecting 1 compared with C_m^s/C' introduces very little error; the error would not be significant for a plot resulting from real values as the experimental uncertainties would be greater than the rounding errors introduced here. Visual inspection of large scale plots of the appropriate data in Table 2 showed curvature only at low values of C_m^s.

Reagent dispersion

The recorder traces are shown in Fig. 4. Values of D_g and D_g^R are given in Table 3 for ten points on each of the two curves. Linear regression on the

TABLE 2

Data for plots of peak width vs. ln (function of concentration)

C_m^s	ln C_m^s	$(C_m^s/C') - 1$	ln $[(C_m^s/C') - 1]$	Δt
10	2.30	4	1.39	0.52
20	3.00	9	2.20	3.76
40	3.69	19	2.94	6.75
50	3.91	24	3.18	7.68
60	4.09	29	4.37	8.44
80	4.38	39	3.66	9.62
100	4.61	49	3.89	10.5
500	6.21	249	5.52	17.0
1,000	6.91	499	6.21	19.8
5,000	8.52	2499	7.82	26.3
10,000	9.21	4999	8.51	29.0

data for Eqn. 6a gave slope 1.10 ± 0.10, intercept −0.40 ± 0.72 and correlation coefficient 0.994. The ± terms are 95% confidence intervals. The corresponding treatment for Eqn. 6b gave slope 0.97 ± 0.07, intercept 0.037 ± 0.095 and correlation coefficient 0.996. In both cases, the 95% confidence intervals for the slope and intercept include the theoretical values of 1 and 0. The experimental data thus fit the theoretical expressions.

The experimental flow rate was measured to be 2.05 ± 0.05 (95% confidence interval) ml min^{-1}.

A plot of D^R vs. D is given in Fig. 5A. This clearly shows the rapid decrease in D^R as D increases from 1 to 3 (so-called low dispersion systems). For D values between 3 and 10 (medium dispersion systems), D^R changes very little.

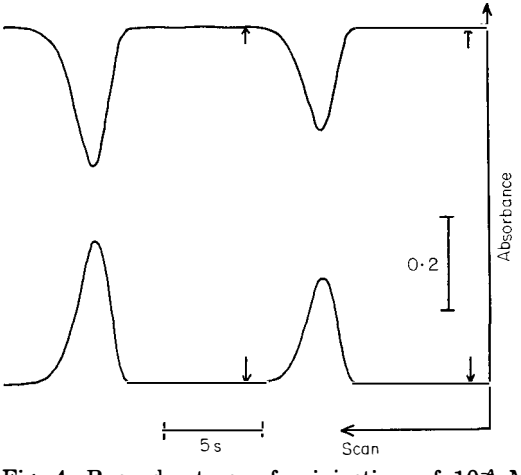

Fig. 4. Recorder traces for injection of 10^{-4} M KNO_3 into water (lower trace) and of water into 10^{-4} M KNO_3 (upper trace). The arrows on the traces show the points of injection.

TABLE 3

Values for D_g and D_g^R obtained from recorder traces shown in Fig. 4 and the corresponding calculated values based on Eqn. 6 (the measured values of C_m^s and C_m^R were both 191 mm)

C_g^s (mm)	D_g	$D_g/(D_g-1)$	C_g^R (mm)	D_g^R	$D_g^R/(D_g^R-1)$
26.0	7.35	1.16	167.7	1.14	8.14
55.5	3.44	1.41	135.7	1.41	3.43
23.8	8.03	1.14	164.6	1.16	7.25
21.2	9.01	1.12	167.8	1.14	8.24
76.8	2.49	1.67	116.1	1.65	2.55
44.5	4.29	1.30	145.0	1.32	4.15
11.5	16.61	1.06	178.0	1.07	15.3
56.6	3.37	1.42	135.5	1.41	3.44
35.5	5.38	1.23	157.5	1.21	5.70
64.5	2.96	1.51	125.0	1.53	2.89

As it is the values of D and D^R which govern the peak concentrations of sample and reagent, respectively (for any given initial concentrations), it is of interest to see how the ratio of peak concentrations varies with D. If $R^{R/s}$ is the ratio of reagent to sample, then at the peak maximum $R_p^{R/s} = C_p^R/C_p^s$, and substituting from Eqns. 2, 3 and the peak version of 6b gives

$$R_m^{R/s} = R_p^{R/s}/(D-1) \tag{13}$$

The relationship between $R_m^{R/s}$ and D is illustrated in Fig. 5B for the case where $R_p^{R/s}$ is 10. It can be seen from this plot (and from Eqn. 13) that provided $D > 2$, then $R_m^{R/s} < R_p^{R/s}$; i.e., if a desired concentration ratio is required at the peak maximum to obtain a particular degree of reaction, it is not necessary to have as high a ratio between the reagent carrier and injected sample. For example, in this case, if the value of D was 5, an initial concen-

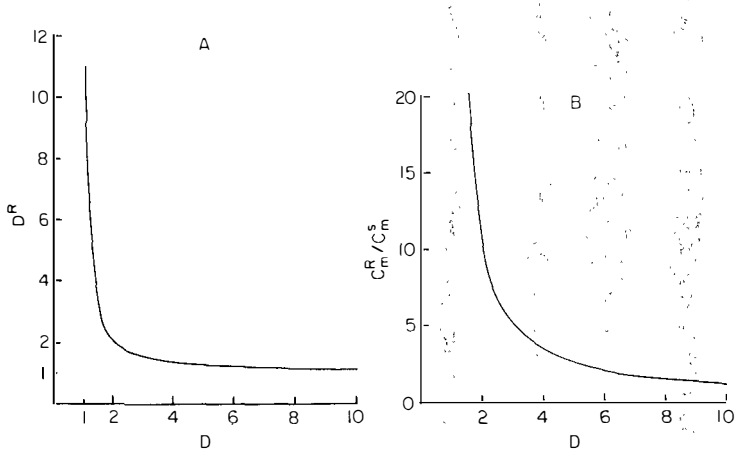

Fig. 5. Relationship between D^R and D (curve A) and C_m^R/C_m^s and D (curve B). For curve B, a value of C_p^R/C_p^s of 10 was taken.

tration ratio of 2.5 produces a peak concentration ratio of 10. To maximize the advantage to be obtained from this relationship (i.e., to economize on reagent as much as possible) requires a large value of D which in turn reduces the sensitivity.

The use of the reversed f.i.a. configuration (injection of reagent into sample) has been claimed as a means of increasing the sensitivity [15]. The basis of this claim may be examined by applying the relationships derived above. In the example discussed, it is required that at the peak maximum the sample material shall be diluted to not more than 0.8 times its original concentration and that to obtain the required degree of reaction a 10-fold excess of reagent is required at the peak maximum. For conventional f.i.a., D must be $1/0.8 = 1.25$ and thus, from Eqn. 13 a 40-fold concentration excess of reagent (over the sample concentration) is needed in the carrier stream. For reversed f.i.a., a value of D (based on injected material dispersion) of 5 is required and again a 40-fold concentration excess of reagent (injected) to sample (in the carrier stream) is required. On the basis of the single-line well stirred mixing chamber model for dispersion behaviour, if $V = 100$ µl then to obtain $D = 1.25$ for conventional f.i.a. the volume injected needed can be calculated from Eqn. 12 to be 161 µl. For reversed f.i.a., the volume injected required is 22 µl. At first sight it would appear that the theoretical sampling frequency for reversed f.i.a. will be higher than for conventional f.i.a. for manifolds which achieve comparable sensitivity. However, it should be borne in mind that the peak-width at the baseline is set by the time taken for the product concentration to reduce to some acceptable value, say 0.03, of the peak value. In conventional f.i.a., the product profile follows the sample profile and thus on the basis of the well stirred mixing chamber model, the baseline peak-width is calculated to be 15 s. In the case of reversed f.i.a., the product profile follows the injected reagent profile. As in this example, the reagent is 10-fold more concentrated at the peak than the sample, the product profile returns to within the same value of the baseline as for the conventional f.i.a. case when the reagent concentration has fallen to 0.003 of its peak value, giving a total width of 18 s. Of course, if discrete samples are used in reversed f.i.a., the sampling frequency is limited. However, reversed f.i.a. does conserve reagent and, for the identical manifold (including volume injected), is more sensitive.

Dispersion and chemical reaction

Typical double peaks are shown in Fig. 6A, the results for the peak separations for the range 0.1—10 000 mg l^{-1} are given in Table 4, and a plot of Δt_{eq} vs. ln C_m^s is shown in Fig. 6B. The line shown is the best fit on the basis of linear regression. The results for this were slope 2.89 ± 0.50 s, intercept 11.4 ± 2.6 s and correlation coefficient 0.992. From the flow rate of 2.05 ± 0.05 ml min^{-1} and the slope of the plot, the volume, V, of the equivalent mixing chamber is calculated to be 99 ± 17 µl and the dispersion coefficient as 1.008 ± 0.006. From the intercept, $-(V/u^s) \ln C_m^R (D - 1)$, the dispersion

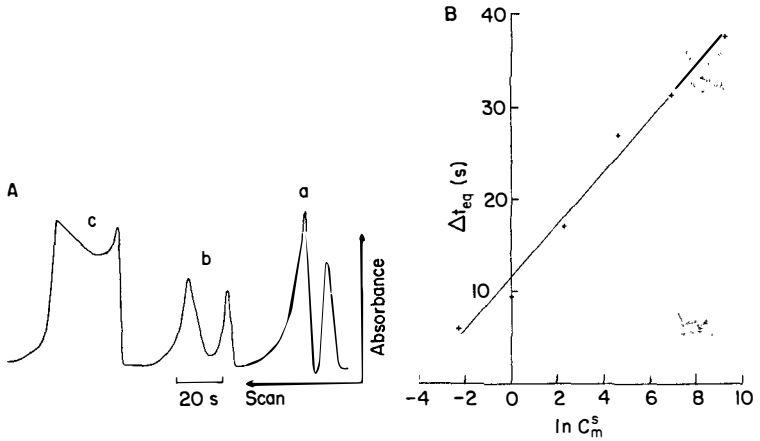

Fig. 6. Peak width when reagent concentration is deficient. A, The recorder traces obtained when 500 μl of 1, 10 and 100 mg l^{-1} Cu^{2+} (traces a, b and c) were injected into a 10^{-4} M EDTA carrier stream (the vertical scale is not the same for all peaks); the minimum between the peaks decreases as the Cu^{2+} injected increases because Cu^{2+} absorbs at the wavelength used. B, A plot of peak width against natural logarithm of the injected concentration.

TABLE 4

Results for peak-width (separation between doublets) as a function of injected concentrations (carrier 10^{-4} M EDTA, sample Cu^{2+})

C_m^s (mg l^{-1})	ln C_m^s	Δt_{eq} (s)	Baseline to baseline peak-width[a] (s)
0.1	−2.303	6.0	21
1	0	9.5	28
10	2.303	17.0	35
100	4.605	27.0	41
1000	6.908	31.2	48
10 000	9.210	37.5	55

[a]Calculated values on the basis of the well-stirred mixing chamber model.

coefficient is calculated to be 1.009 ± 0.007. (All the deviations given are for 95% confidence intervals.)

Taking 0.01 mg l^{-1} as the level indistinguishable from the baseline, the base-widths can be estimated from Eqn. A1.9 (see Appendix 1) and values of V_i, V and u for the above experiment. The results of the calculation are shown in Table 4. Thus the base-width increases by about 7 s for every 10-fold increase in sample concentration as does the doublet peak separation. Thus five orders of magnitude change in concentration can be accommodated on one calibration graph without the base-width becoming impractically large. As time measurements may be made, with fairly simple data logging

equipment, to the nearest 0.01 s [14] and precisions of well under 1% RSD may be obtained, it should be possible to distinguish between small relative differences in concentration. At high concentrations of analyte, this may provide a satisfactory measurement of the analyte concentration or, if not, it will give the dilution factor required to bring the concentration onto a more accurate restricted range calibration. For low concentrations of analyte compared with reagent, such a calibration may be obtained from the doublet peak chart recording with no further experimental work other than measuring peak height.

The reason for this is embodied in Eqn. 8. If essentially complete reaction is assumed, C_{eq} represents the product concentration at the peak maximum. The way in which this is related to sample concentration C_m^s is illustrated in Fig. 7 for a reagent concentration of 10^{-4} M. It can be seen from Fig. 7 that, assuming that peak height could be measured, almost linear calibrations would be obtained over the ranges 0—10^{-8} M, 0—10^{-7} M, 0—10^{-6} M and 0—10^{-5} M. The calibration would be curved over the range 0—10^{-4} M but probably usable. However, above 10^{-4} M all peaks have almost the same height and peak height could no longer be used as a quantitative parameter. The reason for this can be seen from Eqn. 8; when $C_m^s > C_m^R$ so that C_m^R can be neglected in comparison, then $C_{eq}^s \approx C_m^R$, and when C_m^s can be neglected in comparison with C_m^R ($C_m^s < C_m^R$), $C_{eq}^s \approx C_m^s$.

CONCLUSIONS

The derivation of equations relating peak-width to concentration for the peak shapes produced by passage through a well stirred mixing chamber

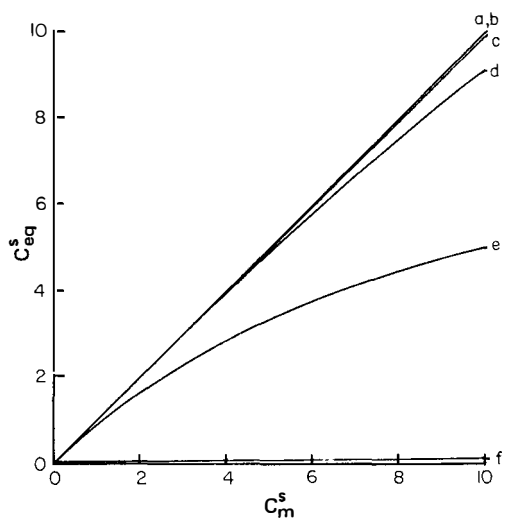

Fig. 7. Plots of C_{eq}^s against C_m^s according to Eqn. 8 for $C_m^R = 10^{-4}$. Curves (a)—(f) cover the ranges 0—10^{-8}, 10^{-7}, 10^{-6}, 10^{-5}, 10^{-4}, 10^{-3}, respectively.

needs no approximations or simplifications. In the absence of chemical reaction, peak-width is not simply a logarithmic function of concentration but a function which approximates very closely to it. For the case in which chemical reaction occurs, the simple ln(concentration) relationship is exact (but only for the single-line manifold). For the merging stream manifold, an equation similar to the case for no chemical reaction applies and a similar approximation may be made to restore the ln(concentration) relationship. The concept of reagent dispersion coefficient is useful in deriving the equations for the case involving chemical reaction and may be applied to other situations in f.i.a., as the relationship with dispersion coefficient is independent of peak shape. Together with the single mixing chamber model of dispersion behaviour, the reagent dispersion coefficient can be used to predict the performance of particular manifolds for systems based on both normal f.i.a. and reversed f.i.a., i.e., the model may be usefully applied to manifolds which do not contain a real mixing chamber.

The peak-width mode in which the reagent concentration is deficient at the centre of the profile has a number of features capable of exploitation for analytical purposes, particularly when the reaction product is monitored rather than one of the reactants. The product peaks occur when the equivalence condition is achieved in the flowing stream and thus there is no difficulty in locating the time values associated with this condition. The only limit to the lowest concentration detectable by this method is set by the ability of the detector to distinguish the product profile from the baseline. Equivalence points can always be achieved by injecting a large enough volume. As this produces a low dispersion coefficient, some caution is needed in the use of terms such as "high dispersion" to describe peak-width methods in f.i.a. The peaks are broader than those obtained in conventional peak-height f.i.a. but the method covers a much wider range of concentrations, so that dilution and re-injection of off-range samples are avoided. The double-peak mode is not restricted to samples of greater concentration than the reagent and contains information to allow peak height to be used as a quantitative parameter, if desired, when the sample concentration is less than the reagent concentration.

This method has considerable potential for investigating chemical reactions, as a manifold designed to give peaks on a scale of minutes or even hours could be used to provide information about the stoichiometry of a reaction and the deviation of the product profile from the theoretically expected profile could be used to calculate the equilibrium constant of the reaction. Each rise and fall of the sample profile provides information analogous to that obtained from the various methods available for determining equilibrium constants (e.g., Job's method, mole-ratio method, Bjerrum's method [16]). A variety of detectors in series could give essentially simultaneous monitoring of a variety of species in the solution.

Financial support from the SERC to purchase the PU4020 detector is gratefully acknowledged.

APPENDIX 1. Physical dispersion in a well stirred mixing chamber

The basis of this model for dispersion behaviour is that the injected plug is transported undispersed to the mixing chamber and that no further dispersion occurs between the mixing chamber exit and the detector. The resulting C, t profile can be described in three stages.

(1) The injected plug flows into mixing chamber. The change in concentration with time is given by $dC/dt = C^s_m u^s/V - Cu/V$. Separating the variables and integrating gives $\ln (C^s_m - C) = -u^s t/V + k$, where k is a constant of integration which may be found, from substituting the initial conditions $C = 0, t = 0$, to be $\ln C^s_m$. Thus

$$t = (V/u^s) \ln [C^s_m/(C^s_m - C)] \quad \text{(A1.1)}$$

which can be rearranged to give

$$C = C^s_m[1 - \exp(-u^s t/V)] \quad \text{(A1.2)}$$

(2) The trailing edge of plug enters the mixing chamber. At this instant, t_p, the concentration in the tank is at its maximum and C^s_p is given by substituting $t_p = V_i/u^s$ in Eqn. A1.2:

$$C^s_p = C^s_m[1 - \exp(-V_i/V)] \quad \text{(A1.3)}$$

(3) Material washed out of the mixing chamber. The change in concentration with time (from the peak maximum) is given by $dC/dt = -C^s_p(u^s/V)$. Integration as described under (1) gives

$$t = (V/u^s) \ln (C^s_p/C) \quad \text{(A1.4)}$$

Reverting to time measured from when the plug started to enter the mixing chamber gives

$$t - t_p = (V/u^s) \ln (C^s_p/C) \quad \text{(A1.5)}$$

which can be rearranged to $C = C^s_p \exp [-u^s(t - t_p)/V]$.

The time interval, Δt, between any two points on the rise and fall curves corresponding to C' can be calculated from $\Delta t = (t_p - t_1) + (t_2 - t_p)$ (see Fig. A1a). Substituting for t_p and t, from Eqn. A1.1 and $(t_2 - t_p)$ from Eqn. A1.5 gives

$$\Delta t = (V_i/u^s) - (V/u^s) \ln [C^s_m/(C^s_m - C')] + (V/u^s) \ln (C^s_p/C')$$

As $D = C^s_m/C^s_p$, rearrangement of Eqn. A1.3 gives

$$D = [1 - \exp(-V_i/V)]^{-1} \quad \text{(A1.6)}$$

and

$$V_i = V \ln [D/(D-1)] \quad \text{(A1.7)}$$

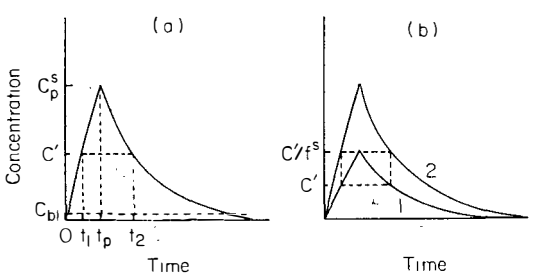

Fig. A1. (a) Concentration profile produced by plug flow through a well stirred mixing chamber. (b) Concentration profile of (1) sample after confluence point and (2) before confluence point. The product profile follows curve 1.

Thus

$$\Delta t = (V/u^s) \ln [D/(D-1)] - (V/u^s) \ln [C_m^s/(C_m^s - C')] + (V/u^s) \ln (C_m^s/DC')$$

which simplifies to

$$\Delta t = (V/u^s) \ln [(C_m^s/C') - 1] - (V/u^s) \ln (D-1) \quad \text{(A1.8)}$$

Other equations for this model. Equation A1.6 gives the dispersion coefficient. Reagent dispersion coefficient is obtained from Eqn. A1.7, i.e., $D^R = \exp(V_i/V)$. The base-width, Δt_b, may be calculated as the time interval between the two points corresponding to a concentration indistinguishable from the baseline, C_{bl} (see Fig. A1a). A value of $C_{bl} > 0$ is necessary, otherwise the washout time is infinite.

An approximate value for the base-width may be obtained by considering it to be made up of the time to the peak maximum, t_p, plus the wash-out time given by $(V/u^s) \ln (C_p^s/C_{bl})$ obtained from Eqn. A1.4:

$$\Delta t_b = (V_i/u) + (V/u^s) \ln (C_p^s/C_{bl}) \quad \text{(A1.9)}$$

An accurate equation is obtained by substitution of C_{bl} for C' in Eqn. A1.8.

APPENDIX 2. Merging stream manifold with reagent concentration always in excess of sample concentration

The manifold is shown in Fig. 1B and the concentration profiles in Fig. 2C. It is assumed that complete reaction occurs so that the product profile is the dispersed sample profile before reaction. The effect of merging the effluent of the mixing chamber with another stream is to dilute both streams. If u^s and u^R are the flow rates of sample and reagent streams, respectively, then the sample is diluted by a factor $(u^s + u^R)/u^s$ at the confluence point and the reagent by a factor $(u^s + u^R)/u^R$. These reciprocals of these factors are referred to as f^s and f^R, respectively. To derive the equation for the peak-width, the equation for the corresponding width of the original sample profile is derived (see Fig. A1b). The width at concentration C' on profile 1 corresponds to the width at C'/f^s on profile 2; the dispersion coefficient D for profile 2 corresponds to Df^s for profile 1.

Substituting into Eqn. A1.8 gives

$$\Delta t = (V/u^s) \ln [(f^s C_m^s/C') - 1] - (V/u^s) \ln (Df^s - 1)$$

Thus $\Delta t = (V/u^s) \ln [(C_m^s/C') - 1/f^s] - (V/u^s) \ln (D - 1/f^s)$.

APPENDIX 3. Merging-stream manifold with sample concentration in excess in profile centre

The reagent stream (Fig. 1B) is diluted by a factor of $1/f^R$ and thus for a 1:1 reaction the equivalence condition is achieved when $C^s = C_m^R f^R$. Referring to Fig. A1b, the required peak width is that for the sample profile before the confluence point. As the sample stream is diluted by a factor of $1/f^s$, the required concentration level is $C_m^R f^R/f^s$. The dispersion coefficient of profile 1, D, corresponds to Df^s for profile 2. Making the appropriate substitutions in Eqn. A1.8 gives

$$\Delta t_{eq} = (V/u^s) \ln [(C_m^s f^s/C_m^R f^R) - 1] - (V/u^s) \ln (Df^s - 1)$$

Adding $(V/u^s) \ln (f^R/f^s)$ to the first term on the right-hand side and subtracting it from the second gives

$$\Delta t_{eq} = (V/u^s) \ln [(C_m^s/C_m^R) - (f^R/f^s)] - (V/u^s) \ln [Df^R - (f^R/f^s)]$$

Thus $\Delta t_{eq} = (V/u^s) \ln [(C_m^s/C_m^R) - (u^R/u^s)] - (V/u^s) \ln [Df^R - (u^R/u^s)]$.

APPENDIX 4. Equivalence condition for general stoichiometric ratio

The reaction between sample, S, and reagent, R, is represented as $mR + nS \rightarrow qP$, where P is the product. If the stoichiometric coefficients of the sample and product are not the

same, then this would have to be incorporated into the equations derived in Appendix 2, as it has been assumed that the product concentration profile follows the sample profile exactly. The situation in which the sample is in excess in the profile centre is different, because the equation refers only to the peak width between the equivalence points, which depends on the ratio of m:n and does not involve the ratios m:q or n:q.

When a certain volume of solution contains equivalent amounts of R and S according to the above stoichiometry, then $nC^{R}_{eq} = mC^{s}_{eq}$. For a single-line manifold, the equivalence condition means that the product profile shows a maximum value at

$$C^{s}_{eq} = C^{s}_{m} C^{R}_{m}/[(C^{s}_{m} m/n) + C^{R}_{m}] \quad \text{(A4.1)}$$

This equation, derived from Eqn. 6(b), should be compared with Eqn. 8. Substitution in Eqn. A1.8 gives

$$\Delta t_{eq} = (V/u^{s}) \ln (mC^{s}_{m}/nC^{R}_{m}) - (V/u^{s}) \ln (D - 1)$$

or

$$\Delta t_{eq} = (V/u^{s}) \ln C^{s}_{m} - (V/u^{s}) \ln (D - 1) C^{R}_{m} n/m$$

For the merging-stream manifold the sample equivalence condition C^{s}_{eq} is given by $C^{s}_{eq} = (n/m) C^{R}_{m} f^{R}$. This is equivalent to a concentration on the sample profile prior to merging of $(n/m) C^{R}_{m} f^{R}/f^{s}$, thus the peak width between equivalence points is

$$\Delta t_{eq} = (V/u^{s}) \ln [(mC^{s}_{m}/nC^{R}_{m}) - (u^{R}/u^{s})] - (V/u^{s}) \ln [Df^{R} - (u^{R}/u^{s})]$$

REFERENCES

1 J. Růžička and E. H. Hansen, Anal. Chim. Acta, 145 (1983) 1.
2 J. Růžička, E. H. Hansen and H. Mosbaek, Anal. Chim. Acta, 92 (1977) 235.
3 K. K. Stewart, Anal. Chem., 55 (1983) 931A.
4 H. L. Pardue and B. Fields, Anal. Chim. Acta, 124 (1981) 39, 65.
5 K. K. Stewart and A. G. Rosenfeld, Anal. Chem., 54 (1982) 2368.
6 S. Olsen, J. Růžička and E. H. Hansen, Anal. Chim. Acta, 136 (1982) 101.
7 J. F. Tyson and J. M. H. Appleton, Talanta, 31 (1984) 9.
8 J. Růžička and E. H. Hansen, Anal. Chim. Acta, 106 (1979) 207.
9 J. Janata and J. Růžička, Anal. Chim. Acta, 139 (1982) 105.
10 B. F. Reis, A. O. Jacintho, J. Mortatti, F. J. Krug, E. A. G. Zagatto, H. Bergamin F° and L. C. R. Pessenda, Anal. Chim. Acta, 123 (1981) 221.
11 O. Levenspiel, Chemical Reaction Engineering, 2nd Edn., Wiley, New York, 1972, Chap. 9.
12 J. F. Tyson, Analyst (London), 109 (1984) 319.
13 J. F. Tyson, J. M. H. Appleton and A. B. Idris, Anal. Chim. Acta, 145 (1983) 159.
14 M. A. Koupparis, P. Anagnostopoulou and H. V. Malmstadt, Talanta, 32 (1985) 411.
15 K. S. Johnson and R. L. Petty, Anal. Chem., 54 (1982) 1185.
16 J. Inczedy, Analytical Applications of Complex Equilibria, Horwood, Chichester, 1976, pp. 89—181.